

This is the accepted manuscript made available via CHORUS. The article has been published as:

Hole polarons and p-type doping in boron nitride polymorphs

L. Weston, D. Wickramaratne, and C. G. Van de Walle

Phys. Rev. B **96**, 100102 — Published 29 September 2017

DOI: [10.1103/PhysRevB.96.100102](https://doi.org/10.1103/PhysRevB.96.100102)

Hole polarons and p -type doping in boron nitride polymorphs

L. Weston, D. Wickramaratne and C. G. Van de Walle

Materials Department, University of California, Santa Barbara, California 93106-5050, USA

(Dated: August 28, 2017)

Boron nitride polymorphs hold great promise for integration into electronic and optoelectronic devices requiring ultra-wide band gaps. We use first-principles calculations to examine the prospects for p -type doping of hexagonal (h -BN), wurtzite (wz -BN) and cubic (c -BN) boron nitride. Group-IV elements (C, Si) substituting on the N site result in a deep acceptor, as the atomic levels of the impurity species lie above the BN valence-band maximum. On the other hand, group-II elements (Be, Mg) substituting on the B site do not give impurity states in the band gap; however, these dopants lead to the formation of small hole polarons. The tendency for polaron formation is far more pronounced in h -BN compared to wz -BN or c -BN. Despite forming small hole polarons, Be acceptors enable p -type doping, with ionization energies of 0.31 eV for wz -BN and 0.24 eV for c -BN; these values are comparable to the Mg ionization energy in GaN.

PACS numbers: 61.72.Bb, 61.72.uj, 71.55.Eq

Boron nitride (BN) polymorphs are candidate materials for use in ultra-wide-band-gap electronics and optoelectronics applications. The most stable crystal structure is the layered hexagonal phase (h -BN),¹ with a band gap close to 6 eV.² Photoluminescence measurements suggest that h -BN is an extremely bright light emitter,³ due to a large exciton binding energy.⁴ While the luminescence efficiency is very high under photoexcitation, the development of devices such as light-emitting diodes or laser diodes requires electrical injection, and doping of the material has proved difficult. In 2011, it was reported that h -BN grown by metal organic chemical vapor deposition (MOCVD) could be doped *in-situ* by Mg, with a hole concentration around 10^{18} cm^{-3} and carrier mobility $\mu = 0.5 \text{ cm}^2/\text{Vs}$ ⁵; however, to date, high-quality p -type doping of h -BN with Mg has not been reproduced by other groups.

High quality doping is crucial for many electronic and optoelectronic applications. Acceptor doping has proved to be particularly problematic for III-nitrides, both due to the lack of suitable dopants and the formation of hole polarons.⁶ In GaN, the development of optoelectronic device technologies has been driven by the success of p -type doping using Mg.^{7,8} While a number of studies have considered doping of BN, for both the bulk^{5,9} and nanostructures,^{10–13} it is still an open research question whether successful p -type doping can be achieved in h -BN.

BN can also crystallize in other phases. It exhibits a cubic phase (c -BN), with the same Bravais lattice as diamond.¹⁴ Reproducible p -type doping in c -BN has been reported,^{15–18} suggesting improved dopability when compared to h -BN. BN can also adopt the wurtzite phase (wz -BN), but reports are scarce. The fabrication of wz -BN is difficult, but has been achieved, for example, using shock compression.¹⁹ The study of wz -BN is most relevant from the point of view of alloying with other III-V nitrides, such as AlN and GaN,²⁰ which provides tunability in the lattice constants and band gap. At low B concentrations, the alloys will crystallize in the wurtzite

structure.

In this Rapid Communication, we use first-principles calculations to investigate p -type doping of BN polymorphs. Our calculations are based on density functional theory (DFT) with a hybrid functional, which provides an accurate treatment of defect transition levels in semiconductors.²¹ In addition, the hybrid functional provides a reliable description of carrier localization, which is essential for the evaluation of small polaron formation²²; such effects are not captured by local or semilocal functionals.

Our results will show that p -type doping in h -BN is not possible due to the formation of small hole polarons, which increases the acceptor ionization energy to more than 1 eV. On the other hand, the c -BN and wz -BN polymorphs can be doped p type. Our calculated acceptor ionization energy for Be in c -BN and wz -BN is comparable to that of Mg in GaN. Therefore, c -BN and wz -BN are promising materials for ultra-wide band-gap electronics and optoelectronics applications requiring p -type doping. Our results elucidate the coupling of polaron physics to the details of the atomic and electronic structure.

Our calculations use DFT within the generalized Kohn-Sham scheme.²³ We use the screened hybrid functional of Heyd, Scuseria and Ernzerhof (HSE).^{24,25} The screening length for the exchange potential is fixed at 10 Å, and the mixing parameter is set to $\alpha = 0.31$, a value which closely reproduces the experimental band gap of h -BN, and provides highly accurate structural parameters for all of the BN polymorphs; moreover, it is similar to the values of α that reproduce the experimental gap of GaN and AlN.²⁶ Our calculated band gaps and lattice constants are presented and compared with experiment in Table I. Van der Waals interactions are included in the case of layered h -BN using the Grimme scheme.²⁷ The valence electrons are separated from the core by use of projector-augmented wave (PAW) potentials²⁸ as implemented in the Vienna *Ab initio* Simulation Package (VASP).²⁹ B $2s^2 2p^1$, N $2s^2 2p^3$, C $2s^2 2p^2$, Si $3s^2 3p^2$, Be

TABLE I: Bulk properties of boron nitride polymorphs. The present HSE-calculated results are compared with experimental values where available.

		a (Å)	c (Å)	E_g (eV)	Ref.
h	Calc.	2.49	6.55	5.94	
	Exp.	2.50	6.65	6.08	2,30
wz	Calc.	2.53	4.19	6.86	
	Exp.	2.55	4.20		19
c	Calc.	3.59		6.15	
	Exp.	3.52		6.36	19,31

$2s^2$ and Mg $3s^2$ electrons are treated as valence. For the h -BN, wz -BN, and c -BN primitive cells, we use $9 \times 9 \times 3$, $9 \times 9 \times 6$, and $9 \times 9 \times 9$ k -point grids, respectively; for the supercells used in defect calculations we use a sampling of the Brillouin zone with comparable density. An energy cutoff of 500 eV was used for the plane-wave basis set. Spin polarization was taken into account.

Defects are simulated using a 240-atom supercell for h -BN and wz -BN, and a 216-atom supercell for c -BN. To construct the supercells for h -BN and wz -BN, we perform a change of basis on the four-atom primitive cell, leading to a new four-atom cell with orthorhombic symmetry. Based on this orthorhombic unit cell we then construct a $5 \times 6 \times 2$ supercell, which has 240 atoms and dimensions $12.94 \text{ Å} \times 12.45 \text{ Å} \times 13.11 \text{ Å}$. The supercell lattice vectors are fixed to the HSE-calculated equilibrium values for the respective polymorphs. The internal coordinates are relaxed until all forces are less than 0.01 eV/Å . Defect formation energies and transition levels are calculated using established methodologies.²¹ For an acceptor impurity A with charge state q the formation energy $E^f[A^q]$ is calculated as:

$$E^f[A^q] = E_{\text{tot}}[A^q] - E_{\text{tot}}[\text{BN}] - \sum_i n_i \mu_i + q \cdot E_F + \Delta^q, \quad (1)$$

where $E_{\text{tot}}[A^q]$ is the total energy of the supercell containing A^q , and $E_{\text{tot}}[\text{BN}]$ is the total energy of the defect-free supercell. n_i represents the number of atoms of species i that are added to ($n > 0$) or removed from ($n < 0$) the supercell, and the chemical potential μ_i represents the energy associated with the reservoir with which the atomic species are exchanged. The electron chemical potential is given by the position of the Fermi level (E_F), referenced to the valence-band maximum (VBM). Finally, the term Δ^q is the charge-state dependent correction due to the finite size of the supercell.³²

The charge-state transition level $\varepsilon(q/q')$ is defined as the Fermi-level position below which the defect is stable (i.e., has the lowest formation energy) in the charge state q , and above which it is stable in charge state q' . For the specific case of the $(0/-)$ transition that determines the

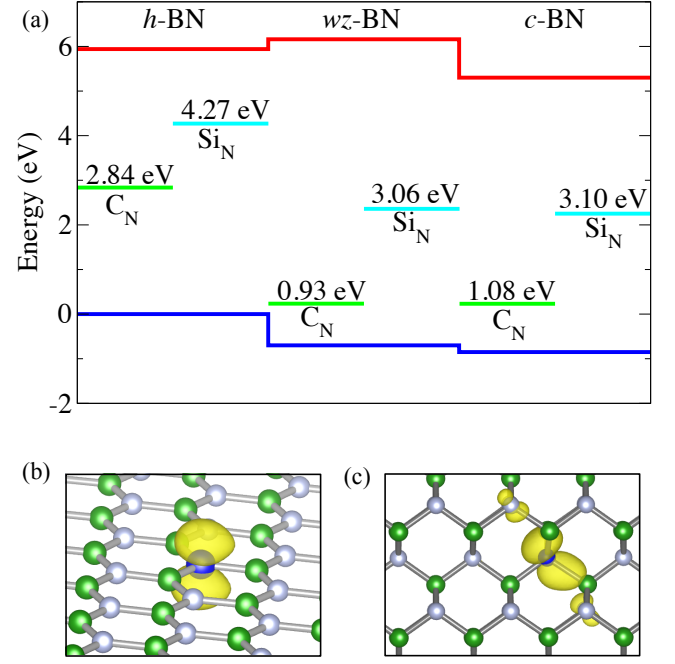


FIG. 1: (a) Charge-state transition levels $\varepsilon(0/-)$ for C and Si acceptors substituting on the N site in BN polymorphs. The band alignments are taken from Ref.³³ Zero energy in the plot is set to the VBM of h -BN. (b) and (c) Spin-density isosurfaces for the neutral C acceptor (C_N^0) in h -BN (b) and c -BN (c). The hole is localized on a C $2p$ state. Green spheres represent B atoms, white N, and blue C.

ionization energy of acceptors:

$$\varepsilon(0/-) = E^f(A^-; E_F = 0) - E^f(A^0), \quad (2)$$

where $E^f(A^-; E_F = 0)$ is the formation energy of A^- when the Fermi level is at the VBM (i.e., for $E_F = 0$). In principle, the μ_i appearing in the formation energy [Eq. 1] are variables that can be chosen to represent experimental conditions; however, the $\varepsilon(0/-)$ levels that are the focus of the present study do not depend on μ_i .

Acceptor doping of BN can be achieved with group-IV elements substituting on the N site, or group-II elements substituting on the B site. For substitution on the N site we consider C and Si (C_N , Si_N), which are expected to have an acceptable size mismatch with the N atom; Ge or other group-IV elements would lead to larger strains and are thus likely unfavorable.³⁴ For substitution on the B site we study Be and Mg (Be_B , Mg_B).

The charge-state transition levels $\varepsilon(0/-)$ for C_N and Si_N , as calculated using Eq. (2), are presented in Fig. 1. In this figure, the band edges of the polymorphs are aligned according to Ref. [33], with the zero of energy set at the VBM of h -BN. Substitutional impurities on the N site clearly lead to the formation of deep acceptor levels, with the $\varepsilon(0/-)$ levels for Si_N being systematically deeper for C_N . The values of $\varepsilon(0/-)$ are very similar in the wurtzite and cubic polymorphs; this is to

be expected, based on the similarity of the local atomic environment in these two phases. These results clearly show that C or Si doping cannot lead to p -type conductivity in BN polymorphs.

C_N and Si_N fall into a class of dopants characterized by the atomic levels of the impurity within the band gap, as previously discussed for other III-nitrides.⁶ Valence-band states, and the acceptor states derived from them, mainly reflect the character of the anion p -states in a compound semiconductor.³⁵ When a dopant impurity substitutes on the anion site, the resulting acceptor level will reflect the energetic position of the impurity p states relative to the energy of the N p states (which make up the VBM). Figures 1(b) and (c) show the spin-density isosurface associated with the neutral C_N^0 impurity in h -BN and c -BN. The hole introduced by the impurity is localized in a C atom $2p$ state, and hence the $\varepsilon(0/-)$ level is determined by the energetic position of the C $2p$ states with respect to the N $2p$ valence band. C $2p$ states are higher in energy than the valence states,³⁵ leading to the transition level being deep in the gap. An analysis of the electronic structure for the Si_N impurity reveals similar results, and the location of the $\varepsilon(0/-)$ level deeper in the band gap reflects the relative ordering of Si and C $2p$ states.

The transition levels for Be and Mg acceptors substituting on the B site are presented in Fig. 2. In h -BN, both Be_B and Mg_B form very deep levels; the ionization energies of 1.15 eV and 1.35 eV are too large to lead to p -type doping in h -BN. The nature of the Be_B and Mg_B acceptor states is different from the states for C_N and Si_N discussed above. Be and Mg substitute on the B site, while valence-band (and hence acceptor) states are associated with the N site. In a compound such as BN, the B cation supplies the electrons that fill the N-derived valence states. Since Be and Mg have one fewer valence electron than B, the missing electron leads to a hole in the valence band. In order for the acceptor to be shallow, this hole should be delocalized. However, the highly localized nature of the N $2p$ states in h -BN leads to a tendency for charge localization, manifested in the formation of small hole polarons.

For the neutral Be_B^0 and Mg_B^0 defects, the localized hole is not found on the impurity atom, but rather on a N host atom adjacent to the impurity. Figure 2(b) shows the spin-density isosurface for the small-polaron state associated with Mg_B^0 in h -BN: the hole is localized on a N atom. The VBM is composed of π -bonding states, and one of these states has localized onto a single N p_z orbital, accompanied by a lattice distortion. The charge localization lowers the energy of the neutral charge state of the impurity with respect to that of the negative charge state, and therefore pushes the $\varepsilon(0/-)$ level deeper into the gap [Eq. (2)]. This type of small-polaron formation was identified as the origin of the deep acceptor levels in other III-nitrides,⁶ as well as in various oxides.^{6,22,36} Our calculations indicate this does not occur in the pure bulk material, but the presence of a perturbation such as an acceptor impurity stabilizes the hole polaron.

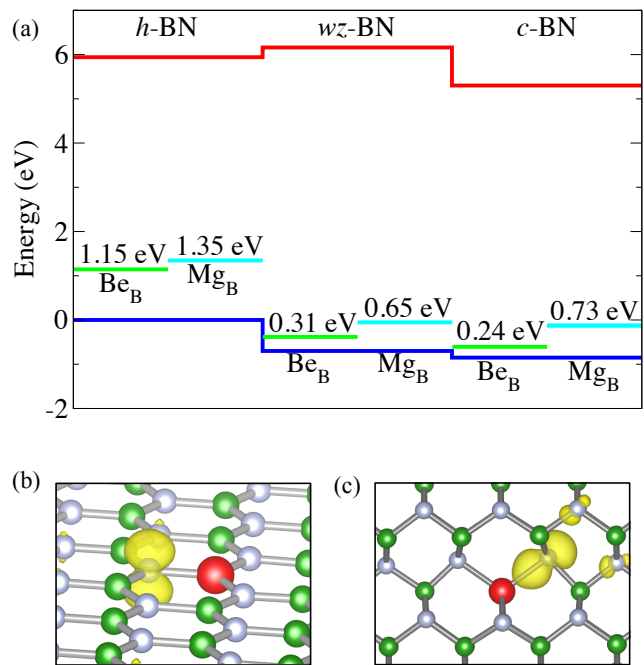


FIG. 2: (a) Charge-state transition levels $\varepsilon(0/-)$ for Be and Mg acceptors substituting on the B site in BN polymorphs. The band alignments are taken from Ref.³³ Zero energy in the plot is set to the VBM of h -BN. (b) and (c) Spin-density isosurfaces for the neutral Mg acceptor (Mg_B^0) in h -BN (b) and c -BN (c). The hole is localized on a N $2p$ state in the form of a small polaron. Green spheres represent B atoms, white N, and red Mg.

In contrast to h -BN, we find that the Be_B and Mg_B $\varepsilon(0/-)$ levels are much closer to the VBM in the wz -BN and c -BN polymorphs [Fig. 2(a)]. Again, the values of $\varepsilon(0/-)$ are very similar in wurtzite and cubic. Small-polaron formation still occurs in the neutral charge state, as evidenced by the spin-density isosurface in Fig. 2(c). We can understand the difference between h -BN, on the one hand, and c - and wz -BN, on the other hand, based on the different bonding character. h -BN exhibits sp^2 bonding, with $2p_z$ orbitals perpendicular to the BN planes. Only a small amount of atomic displacement is required to localize a hole in one of these p_z orbitals; i.e., the energy cost for forming the polaron is small, leading to a low energy for the neutral charge state and a large ionization energy. In contrast, wz -BN and c -BN exhibit sp^3 bonding. Localization of a hole requires breaking of a σ bond, which is accomplished mainly by pushing a neighboring N atom outwards towards the plane of its three B neighbors [see Fig. 2(c)]. This displacement costs energy; in fact, BN is among the hardest materials known,^{37,38} and hence the elastic energy cost is high. This cost raises the energy of the neutral charge state, and therefore lowers $\varepsilon(0/-)$ level [Eq. (2)]. The larger the displacement, the less favorable the polaron state, which is indeed the trend we observe for Be: the displacement of the N atom is larger

in *c*-BN than in *wz*-BN, consistent with the smaller ionization energy in the cubic phase.

Our calculated $\varepsilon(0/-)$ levels are systematically deeper than those reported by Oba *et al.* in Ref.⁹; however, spin polarization was not included in those calculations, and therefore the formation of small polarons could not be properly addressed. Oba *et al.*⁹ also proposed that intercalated F atoms could be used to dope *h*-BN *p*-type; however, we find that intercalated F atoms also lead to formation of small polarons, and the associated $\varepsilon(0/-)$ level is 1.18 eV above the VBM.

The formation of deep acceptor levels via hole localization appears to be intrinsic to *h*-BN, and *p*-type doping of this material seems unlikely. This result contradicts the experimental result of Dahal *et al.*,⁵ who reported an acceptor ionization energy for Mg in *h*-BN of 30 meV; however, we note that this result has not been reproduced. The present result shows that the 30 meV acceptor level cannot originate from Mg_N . Our results about the tendency for polaron formation in *h*-BN also make it unlikely that any shallow-acceptor state can be formed in this material; however, we can of course not conclusively rule out that some other Mg-related defect could give rise to the experimental result in Ref.⁵

Our results for the cubic and wurtzite phases, on the other hand, show that *p*-type doping is feasible. The Be_B (0/-) level, in particular, is quite shallow, with an ionization energy similar to that calculated for Mg acceptors in GaN (260 meV).²⁶ Our calculated $\varepsilon(0/-)$ level of 0.24

eV for Be_B in *c*-BN is consistent with the experimentally reported values of 0.22 eV,¹⁸ and 0.19 – 0.23 eV,¹⁵ based on temperature-dependent conductivity measurements.

In summary, using first-principles calculations we have determined the acceptor levels for a number of substitutional species in BN polymorphs. Group-IV elements (C, Si) substituting on the N site lead to atomic-like levels in the band gap for all BN polymorphs, and consequently the acceptor levels are far too deep for *p*-type doping. In the case of Group-II elements (Be, Mg) substituting on the B site hole polarons form on a N atom adjacent to the impurity. In the hexagonal phase, polarons form very deep levels. While polarons also form in the cubic and wurtzite phases, they lead to far lower ionization energies than in *h*-BN. Beryllium doping, in particular, with ionization energies of 0.24 eV in *c*-BN and 0.31 eV in *wz*-BN, provides a promising route to *p*-type conductivity in ultra-wide-band-gap BN.

This work was supported by the National Science Foundation under Grant No. DMR-143485, and by the Center for Low Energy Systems Technology (LEAST), one of six SRC STARnet Centers sponsored by MARCO and DARPA. Computational resources were provided by the Center for Scientific Computing at the CNSI and MRL (an NSF MRSEC, DMR-1121053) (NSF CNS-0960316), and by the Extreme Science and Engineering Discovery Environment (XSEDE), which is supported by NSF Grant No. ACI-1053575.

-
- ¹ R. S. Pease, Acta Crystallogr. **5**, 356 (1952).
 - ² G. Cassabois, P. Valvin, and B. Gil, Nat. Photon. (2016).
 - ³ K. Watanabe, T. Taniguchi, and H. Kanda, Nat. Mater. **3**, 404 (2004).
 - ⁴ B. Arnaud, S. Lebegue, P. Rabiller, and M. Alouani, Phys. Rev. Lett. **96**, 026402 (2006).
 - ⁵ R. Dahal, J. Li, S. Majety, B. Pantha, X. Cao, J. Lin, and H. Jiang, Appl. Phys. Lett. **98**, 211110 (2011).
 - ⁶ J. Lyons, A. Janotti, and C. Van de Walle, J. Appl. Phys. **115**, 012014 (2014).
 - ⁷ S. Nakamura, T. Mukai, M. Senoh, and N. Iwasa, Jpn. J. Appl. Phys. **31**, L139 (1992).
 - ⁸ S. Nakamura, N. Iwasa, M. Senoh, and T. Mukai, Jps. J. Appl. Phys. **31**, 1258 (1992).
 - ⁹ F. Oba, A. Togo, I. Tanaka, K. Watanabe, and T. Taniguchi, Phys. Rev. B **81**, 075125 (2010).
 - ¹⁰ C. Ataca and S. Ciraci, Phys. Rev. B **82**, 165402 (2010).
 - ¹¹ C. Huang, C. Chen, M. Zhang, L. Lin, X. Ye, S. Lin, M. Antonietti, and X. Wang, Nat. Commun. **6** (2015).
 - ¹² Q. Weng, X. Wang, X. Wang, Y. Bando, and D. Golberg, Chem. Soc. Rev. **45**, 3989 (2016).
 - ¹³ Y. Ding, J. Shi, M. Zhang, X. Jiang, H. Zhong, P. Huang, M. Wu, and X. Cao, RSC Adv. **6**, 29190 (2016).
 - ¹⁴ R. Wentorf Jr, J. Chem. Phys. **26**, 956 (1957).
 - ¹⁵ R. Wentorf Jr, J. Chem. Phys. **36**, 1990 (1962).
 - ¹⁶ O. Mishima, K. Era, J. Tanaka, and S. Yamaoka, Appl. Phys. Lett. **53**, 962 (1988).
 - ¹⁷ M. Lu, A. Boussetta, A. Bensaoula, K. Waters, and J. Schultz, Appl. Phys. Lett. **68**, 622 (1996).
 - ¹⁸ T. Taniguchi, S. Koizumi, K. Watanabe, I. Sakaguchi, T. Sekiguchi, and S. Yamaoka, Diamond Relat. Mater. **12**, 1098 (2003).
 - ¹⁹ T. Sōma, A. Sawaoka, and S. Saito, Mater. Res. Bull. **9**, 755 (1974).
 - ²⁰ T. Akasaka and T. Makimoto, Applied physics letters **88**, 1902 (2006).
 - ²¹ C. Freysoldt, B. Grabowski, T. Hickel, J. Neugebauer, G. Kresse, A. Janotti, and C. G. Van de Walle, Rev. Mod. Phys. **86**, 253 (2014).
 - ²² J. Varley, A. Janotti, C. Franchini, and C. Van de Walle, Phys. Rev. B **85**, 081109 (2012).
 - ²³ W. Kohn and L. J. Sham, Phys. Rev. **140**, A1133 (1965).
 - ²⁴ J. Heyd, G. Scuseria, and M. Ernzerhof, J. Chem. Phys. **118**, 8207 (2003).
 - ²⁵ J. Heyd, G. E. Scuseria, and M. Ernzerhof, J. Chem. Phys. **124**, 219906 (2006).
 - ²⁶ J. L. Lyons, A. Janotti, and C. G. Van de Walle, Phys. Rev. Lett. **108**, 156403 (2012).
 - ²⁷ S. Grimme, J. Antony, S. Ehrlich, and H. Krieg, J. Chem. Phys. **132**, 154104 (2010).
 - ²⁸ P. E. Blöchl, Phys. Rev. B **50**, 17953 (1994).
 - ²⁹ G. Kresse and J. Furthmüller, Phys. Rev. B **54**, 11169 (1996).
 - ³⁰ Y. Gu, M. Zheng, Y. Liu, and Z. Xu, J. Am. Ceram. Soc. **90**, 1589 (2007).
 - ³¹ D. Evans, A. McGlynn, B. Towlson, M. Gunn, D. Jones,

- T. Jenkins, R. Winter, and N. Poolton, J. Phys.: Condens. Matter **20**, 075233 (2008).
- ³² C. Freysoldt, J. Neugebauer, and C. G. Van de Walle, Phys. Status Solidi B **248**, 1067 (2011).
- ³³ C. E. Dreyer, J. L. Lyons, A. Janotti, and C. G. Van de Walle, Appl. Phys. Express **7**, 031001 (2014).
- ³⁴ J. Neugebauer and C. G. Van de Walle, J. Appl. Phys. **85**, 3003 (1999).
- ³⁵ W. Harrison, *Elementary electronic structure* (World Scientific Publishing Co Inc, 1999).
- ³⁶ L. Weston, A. Janotti, X. Y. Cui, C. Stampfl, and C. G. Van de Walle, Phys. Rev. B **89**, 184109 (2014).
- ³⁷ Y. Tian, B. Xu, D. Yu, Y. Ma, Y. Wang, Y. Jiang, W. Hu, C. Tang, Y. Gao, K. Luo, et al., Nature **493**, 385 (2013).
- ³⁸ Z. Pan, H. Sun, Y. Zhang, and C. Chen, Phys. Rev. Lett. **102**, 055503 (2009).